



## Research Article

# Experimental Investigation on Converting the Acid Gas of an HDS Unit to High-Value Products by Methanol Thiolation: A Case Study

Mohammad Reza Shabani<sup>1\*</sup>, Sayed Javid Royaei<sup>1\*</sup>, Yahya Zamani<sup>2</sup>, Mohammad Ali Moosavian<sup>3</sup>

<sup>1</sup>Petroleum Refining Technology Department Division, Research Institute of Petroleum Industry, Azadi Sport Complex West Blvd., Tehran, Iran

<sup>2</sup>Gas Research Division, Research Institute of Petroleum Industry, Azadi Sport Complex West Blvd., Tehran, Iran

<sup>3</sup>School of Chemical Engineering, Faculty of Engineering, University of Tehran, Tehran, Iran

E-mail: shabanimr@ripi.ir; royaeesj@ripi.ir

**Received:** 16 October 2022; **Revised:** 19 December 2022; **Accepted:** 6 January 2023

**Abstract:** The possibility of using acid gas as feedstock in a methanol thiolation reaction was examined with  $K_2O/WO_3/\gamma-Al_2O_3$  catalysts, and the effect of impurities on  $H_2S$  conversion and product distribution was evaluated in this paper. The results were compared with the case using pure  $H_2S$  as feedstock. Three samples of catalysts were synthesized by incipient wetness impregnation. The catalysts are characterized by Brunauer-Emmett-Teller, X-ray powder diffraction, and  $NH_3$ -temperature programmed desorption methods. Catalytic tests were performed in a fixed-bed flow reactor for an acid gas with 12.2% mol.  $H_2S$ . Dimethyl sulfide (DMS) and methanethiol are produced through a methanol thiolation reaction, and hydrogen is produced by a hydrocarbon reforming reaction. The catalyst with the lowest acidity showed the best results.  $H_2S$  in acid gas is converted at about 78.6%. The yields were reported at 74.8% and 3.8% for DMS and methanethiol, respectively. The amount of hydrogen increased by more than 200% in the reactor outlet.

**Keywords:** acid gas, methanol thiolation, DMS, methanethiol, catalysts

## Nomenclature

A	catalyst A
As	specific area ( $m^2/g$ )
atm	atmosphere pressure
B	catalyst B
BPD	barrels per day
BET	Brunauer-Emmett-Teller
C	catalyst C
Cs	cesium
DMS	dimethyl sulfide
FID	flame ionization detector
GHSV	gas hourly space velocity ( $hr^{-1}$ )
g	gram

$H_{2,in}$	inlet hydrogen to the reactor (g/min)*10 <sup>3</sup>
$H_{2,out}$	outlet hydrogen from the reactor (g/min)*10 <sup>3</sup>
HC	hydrocarbons
$HC_{in}$	inlet hydrocarbons to the reactor (g/min)*10 <sup>3</sup>
$HC_{out}$	outlet hydrocarbons from the reactor (g/min)*10 <sup>3</sup>
LHSV	liquid hourly space velocity (hr <sup>-1</sup> )
MFC	mass flow controller
MM	methanethiol
MMUS\$	million United States Dollars
MT	methanol thiolation
$n_i$	number of mole of component $i$
$p/p_0$	relative pressure in BET
Rb	rubidium
$S_i$	selectivity of component $i$
SIC	silicon carbide
SRU	sulfur recovery unit
TCD	thermal conductivity detector
TPD	temperature programmed desorption
tph	ton per hour
$V_a$	nitrogen volume adsorbed/desorbed per gram of catalyst (cm <sup>3</sup> , STP)/g
$v_i$	volume flow rate of component $i$ (cm <sup>3</sup> /min)
$X_{H_2S}$	conversion of hydrogen sulfide
XRD	X-ray powder diffraction
$Y_i$	yield of component $i$

## Greek letters

$\theta$	diffraction angle in XRD (degree)
$\gamma$	prefix for gamma alumina

## 1. Introduction

Hydrogen sulfide is a dangerous acid gas that is produced in petroleum and gas refineries by hydrodesulfurization (HDS) units. Hydrodesulfurization is a catalytic chemical process that removes sulfur from natural gas or refined petroleum products such as naphtha, kerosene, and diesel. Sulfur compounds react with hydrogen in a fixed-bed reactor and convert to hydrogen sulfide, along with sulfur-free organic compounds. HDS reactors operate at high temperatures ranging from 573 to 673 K and high pressures ranging from 30 to 130 atm [1, 2]. A schematic diagram of an HDS unit is shown in Figure 1.

Source: Wikipedia

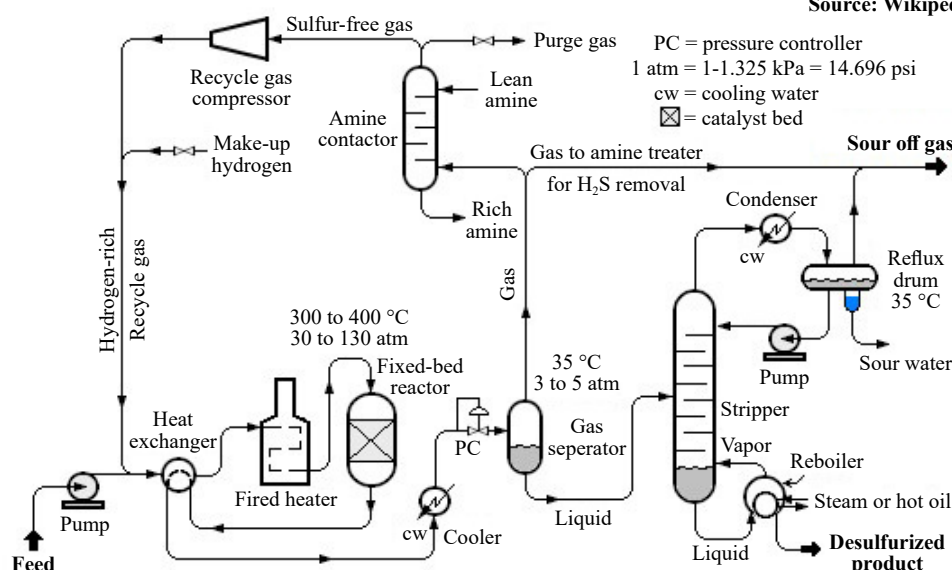


Figure 1. Schematic diagram of a typical HDS unit in a petroleum refinery

Acid gases pose many dangers to human health due to their concentration and exposure level. According to the Occupational Safety and Health Administration (OSHA), H<sub>2</sub>S exposure up to 10 ppm is classified as low-hazard, exposure between 10 ppm and 30 ppm is known as medium-hazard, and exposure higher than 30 ppm is designated as high-risk.

There are several technologies for sulfur recovery from acid gases that use absorption, adsorption, catalytic, and thermal oxidation processes for converting H<sub>2</sub>S to elemental sulfur. The most important sulfur recovery technologies are H<sub>2</sub>S scavengers, liquid redox, biological processes, and the Claus process. The choice of a suitable sulfur recovery technology depends on several factors, including temperature, pressure, gas volume, the type of acid gas, types and concentrations of impurities, air pollution laws, and the amount of capital/operating cost [3]. However, sulfur capacity is the first criterion for screening sulfur recovery technologies (Table 1).

Table 1. Sulfur recovery process technologies, with permission of Gupta et al. [4]

H <sub>2</sub> S content (%)	Treatment process	Sulfur production capacity (kg/s)	Sulfur recovery level (%)
0-100	H <sub>2</sub> S scavengers	< 0.0012-0.0024	92-99.9
0-100	Liquid redox	0.0012-0.0024	95-99.9
0-100	Biological process	0.0012-0.47	92-99.9
1-5	Selectox process	0.0059-0.59	94-99.9
0-100	Recycle selectox	0.0059-0.59	94-99.9
20-100	Claus process	0.035-0.176; > 0.176	90-98

Since elemental sulfur is the final product in almost all sulfur recovery technologies, and due to its low value, the authors encouraged finding a process to convert H<sub>2</sub>S to high-value products.

Conversion of H<sub>2</sub>S to methanethiol can be performed in two methods. In the first method, H<sub>2</sub>S reacts with methanol (the methanol thiolation reaction). This process has been commercialized and can produce some valuable products such as methanethiol, DMS, and dimethyl ether in a fixed-bed reactor loaded with an Alkali/W/Al<sub>2</sub>O<sub>3</sub> catalyst [5-16]. The second method refers to the reaction of H<sub>2</sub>S with syngas (H<sub>2</sub> + CO), which is in the research stage [17-23]. Both reactions use expensive, pure H<sub>2</sub>S as feedstock. Acid gases usually contain a considerable amount of H<sub>2</sub>S and are capable of being used

as the source of H<sub>2</sub>S for methanol thiolation. To test this idea, the acid gas of an HDS unit was investigated as feedstock for the methanol thiolation reaction. K<sub>2</sub>O/WO<sub>3</sub>/Al<sub>2</sub>O<sub>3</sub> catalysts were synthesized and then tested in a fixed-bed reactor. The effect of impurities (hydrogen and hydrocarbons) on H<sub>2</sub>S conversion and product distribution was evaluated.

## 2. Catalyst preparation

The catalysts were prepared by incipient wetness impregnation of  $\gamma$ -Al<sub>2</sub>O<sub>3</sub> in two steps. Before starting impregnation,  $\gamma$ -Al<sub>2</sub>O<sub>3</sub> was heated at 450 °C for 3 hr to remove any water content. In the first step, the aqueous solution of ammonium metatungstate hydrate ((NH<sub>4</sub>)<sub>6</sub>H<sub>2</sub>W<sub>12</sub>O<sub>40</sub>, > 85% WO<sub>3</sub> basis, Exir) was impregnated on  $\gamma$ -Al<sub>2</sub>O<sub>3</sub>. The impregnated solids (WO<sub>3</sub>/ $\gamma$ -Al<sub>2</sub>O<sub>3</sub>) dried at 120 °C for 12 hr and were calcined at 455 °C for 3 hr. In the second step, the aqueous solution of potassium hydroxide (KOH, 85%, Merck) was impregnated on WO<sub>3</sub>/ $\gamma$ -Al<sub>2</sub>O<sub>3</sub> to form K<sub>2</sub>O/WO<sub>3</sub>/ $\gamma$ -Al<sub>2</sub>O<sub>3</sub>. The impregnated solids (K<sub>2</sub>O/WO<sub>3</sub>/ $\gamma$ -Al<sub>2</sub>O<sub>3</sub>) dried at 120 °C for 12 hr and were then calcined at 455 °C for 3 hr. The concentration of solid salts in the impregnation solution was adjusted so that K and W contents (K, W) were A (18.4%, 8.2%), B (8.2%, 18.4%), and C (16.7%, 16.7%) all in mass percent. The prepared catalysts were treated by a stream of H<sub>2</sub>S (10% vol. of H<sub>2</sub>S and 90% vol. of N<sub>2</sub>) for sulfidation. The synthesized catalysts are shown in Table 2.

**Table 2.** Identification of synthesized catalysts

Catalyst	K (mass %)	W (mass %)	Density (g/cm <sup>3</sup> )
A	18.4	8.2	0.86
B	8.2	18.4	0.92
C	16.7	16.7	1.02
$\gamma$ -Al <sub>2</sub> O <sub>3</sub>	0.0	0.0	0.53

## 3. Reactor tests

Catalytic tests are performed in a fixed-bed flow reactor. A schematic of the setup is shown in Figure 2. The tubular reactor with a diameter of 1 in and a length of 1 m has been made of Stainless Steel Grade 321 (SS321). The reactor was placed inside an electrical heater. The catalyst had a cylindrical shape with a diameter of 1 mm and a length of 2 mm. 1 g of catalyst was mixed with 8 g of silicon carbide and loaded into the reactor. SIC is used to dissipate the heat of the reaction and guarantees a constant bed temperature. For in situ activation of catalysts, a stream of 10% vol. H<sub>2</sub>S and 90% vol. N<sub>2</sub> passed over the catalyst bed at 360 °C for 2 hr. There are two feed streams: methanol and acid gas fed to the reactor. Methanol is pumped to the reactor by a reciprocating dosing pump (Model: Eldex). The acid gas stream is charged into the reactor from its cylinder after passing through a mass flow controller. The analysis of the acid gas stream is shown in the next section. The amounts of two feed streams were adjusted so that the molar ratio of CH<sub>3</sub>OH to H<sub>2</sub>S was equal to 2. The liquid hourly space velocity of methanol (LHSV, defined as the volumetric flow of liquid methanol divided by the volume of catalyst) was 0.5 hr<sup>-1</sup>. The reactor effluent was analyzed after 4 hr on stream by online gas chromatography (Model: Agilent 6890) equipped with FID and TCD detectors. Before entering gas chromatography (GC), the effluent stream passed through a series of caustic wash columns. Caustic wash columns filled with 10% wt. caustic solution. The produced methanethiol and unreacted H<sub>2</sub>S were converted to Na<sub>2</sub>S and CH<sub>3</sub>SNa in the caustic solution. The amount of methanethiol and H<sub>2</sub>S was determined by analyzing the caustic wash column's contents with the UOP-163 (Model: KEM510) [24] potentiometric titration test method.

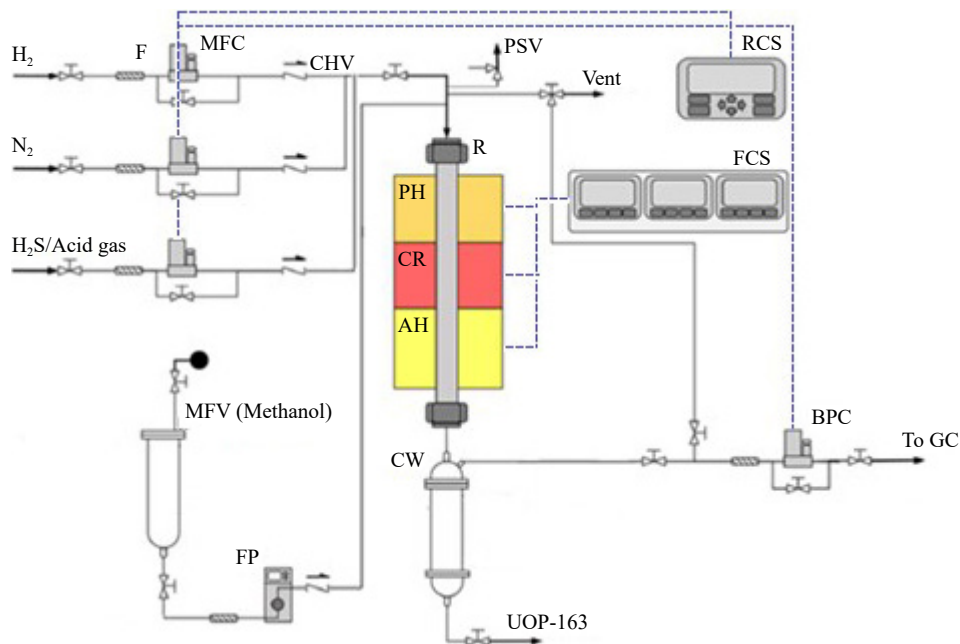


**Figure 2.** Flow scheme of the catalyst performance evaluation system. F: Filter, MFC: Mass flow controller, CHV: Check valve, FP: Feed pump, MFV: Methanol feed vessel, PSV: Pressure safety valve, R: Reactor, PH: Preheater zone, CR: Catalytic reaction zone, AH: After heater zone, CW: Caustic wash vessel, BPC: Back pressure controller, RCS: Readout and controller system, FCS: Furnace controller system, GC: Gas chromatography

## 4. Acid gas specification

The composition of typical acid gas from the naphtha hydrotreater unit in the Lavan refinery (this refinery with a 55,000 BPD capacity is located on Lavan Island in the south of Iran) is shown in Table 3. Hydrogen sulfide has a concentration of 12.2 mol% (19.7 wt%). This stream is selected as a feed stream for the reactor.

**Table 3.** Acid gas composition

Component	mol%	wt%
Hydrogen sulphide	12.2	19.7
Methane	13.3	10.1
Ethane	14.2	20.2
Propane	12.3	25.6
i-Butane	2.5	6.9
n-Butane	5	13.7
Hydrogen	40.5	3.8

## 5. Catalyst characterization

The textural properties of catalysts were determined by the BET method. Specific surface areas were calculated by the BET method, and pore size distributions were determined by  $N_2$  adsorption and desorption isotherms (Belsorbmax at 77 K).

The crystalline structure of catalysts was determined by powder X-ray diffraction utilizing a PW1729 Philips instrument ( $2\theta$  varies between  $2^\circ$  and  $90^\circ$ , Cu lamp: 40 kV, 30 mA with  $1.54 \text{ \AA}$  wavelength).

Total acidic strength and weak/strong acidic sites of catalysts were calculated using ammonia gas by an American

## 6. Results

### 6.1 Catalyst characterization

N<sub>2</sub> adsorption-desorption of catalysts is shown in Figure 3. The textural characteristics of catalysts include the mean pore diameter, total pore volume, and specific surface area (As) given in Table 4. Pore volume and specific surface area decreased by increasing the loading of K and W. Catalysts A and B have the same amount of total loading. The pore diameter of catalyst B is greater than that of catalyst A. The size of the pore diameter is directly related to the amount of tungsten loading.

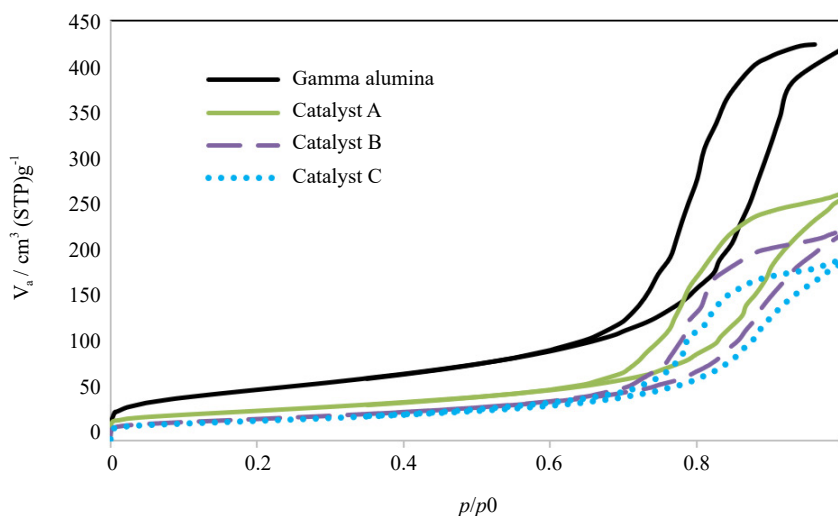


Figure 3. N<sub>2</sub> adsorption-desorption of catalysts

Table 4. Textural properties of catalysts

Catalyst	Mean pore dia. (nm)	Total pore vol. at (p/p0 = 0.99) (cm <sup>3</sup> /g)	As, BET (m <sup>2</sup> /g)
A	14.3	0.39	109.9
B	16.3	0.33	81.9
C	15.6	0.28	73.2
( $\gamma$ -Al <sub>2</sub> O <sub>3</sub> )	13.3	0.64	193.2

$\gamma$ -Al<sub>2</sub>O<sub>3</sub>, WO<sub>3</sub>, K<sub>2</sub>O, and Al<sub>2</sub>O<sub>3</sub>·H<sub>2</sub>O are found in the XRD pattern (Figure 4).  $\gamma$ -Al<sub>2</sub>O<sub>3</sub> has a sharp peak at 2 $\theta$  = 67°, which represents a crystalline structure [25]. The other components did not show any sharp peaks because of the small size or imperfect growth of the crystals.

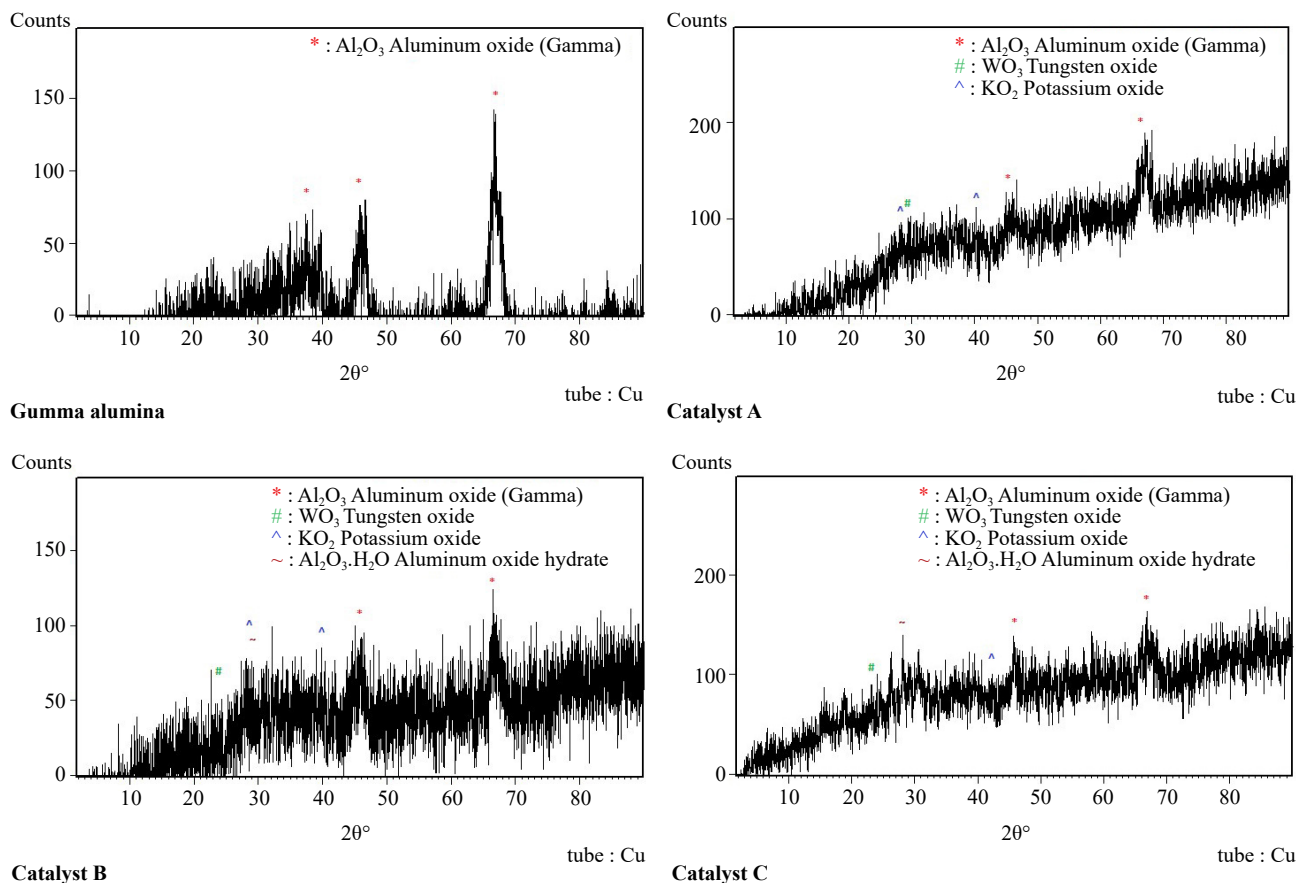


Figure 4. XRD pattern of the catalysts

Ammonia-TPD results show the numbers of weak and strong acid sites as mmol  $\text{NH}_3$  per gram of catalyst. The addition of K and W to  $\gamma\text{-Al}_2\text{O}_3$  diminished the weak acid sites but increased the strong acid sites (Figure 5 and Table 5). The maximum acidity belonged to catalyst B, which has no weak acid sites. The effect of K and W loadings on the acidity of catalysts is shown in Figure 6. Maximum acidity corresponds to maximum W loading (18.4%) and minimum K loading (8.2%). Minimum acidity corresponds to minimum W loading (8.2%) and maximum K loading (18.4%). In general, more W loading results in more acidity due to the existence of acidic  $\text{WO}_3$  particles in the catalyst structure. In addition, more K loading results in less acidity or more basicity due to the existence of basic  $\text{K}_2\text{O}$ .

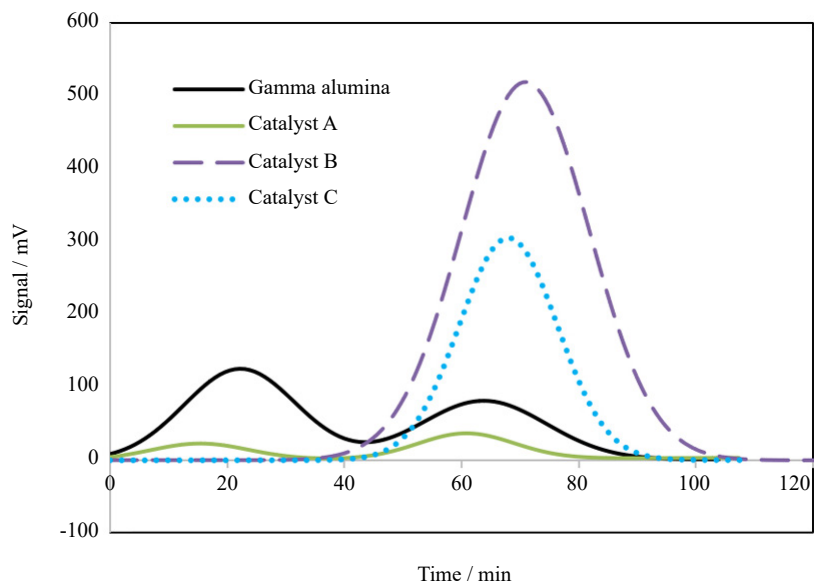


Figure 5. TPD-NH<sub>3</sub> patterns of the catalysts

Table 5. Weak and strong acid numbers

Catalyst	Weak acid sites (Number/ °C)*	Strong acid sites (Number/ °C)*	Total acid sites (Number)**
A	0.09 (166.7)	0.14 (637.5)	0.24
B	0.0	2.84 (747.9)	2.84
C	0.0	1.33 (710.4)	1.33
( $\gamma$ -Al <sub>2</sub> O <sub>3</sub> )	0.68 (234.7)	0.49 (670)	1.17

\*. mmol NH<sub>3</sub> per g catalyst/peak temperature

\*. mmol NH<sub>3</sub> per g catalyst

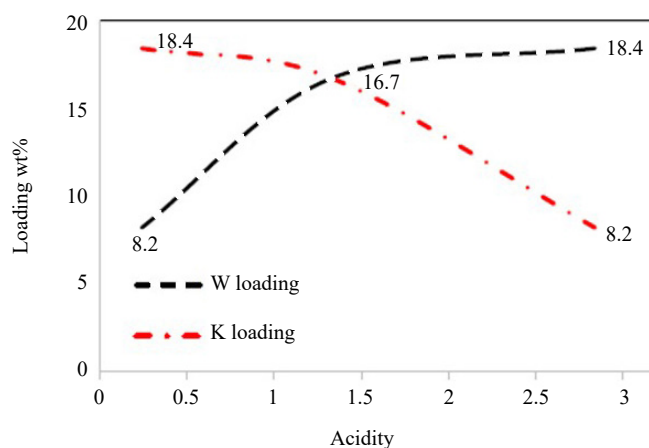


Figure 6. K and W loading effect on acidity

## 6.2 Catalyst activity

The reactor tests were performed for both pure H<sub>2</sub>S and acid gas feeds. Three synthesized catalysts were loaded in



turn. Each catalyst was first sulfided under an H<sub>2</sub>S (10% vol.) and nitrogen (90% vol.) stream for 2 hr in situ. The reactor was run by pure H<sub>2</sub>S and acid gas feeds separately for 4 hr each. All tests were performed with 1 g of catalyst at 360 °C and 1 atm pressure with an LHSV (for liquid methanol) of 0.5 hr<sup>-1</sup> and an H<sub>2</sub>S to methanol molar ratio of 2. The GHSV (gas hourly space velocity, defined as the ratio of gas flow rate at standard conditions to the catalyst volume) is 1508 hr<sup>-1</sup> and 5246 hr<sup>-1</sup> for H<sub>2</sub>S and acid gas feed, respectively. Volumetric flow rates for both feeds are shown in Table 6.

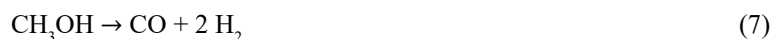
**Table 6.** Volumetric flow rates for the feeds (cm<sup>3</sup>/min.)

Catalyst	Pure H <sub>2</sub> S			Acid gas	
	v <sub>H<sub>2</sub>S</sub>	v <sub>N<sub>2</sub></sub>	v <sub>methanol (liq.)</sub>	v <sub>acid gas</sub>	v <sub>methanol (liq.)</sub>
A	11.7	11.7	0.01	95.8	0.01
B	10.9	10.9	0.01	89.5	0.01
C	9.9	9.9	0.01	80.8	0.01

Methanol thiolation consists of one main reaction between methanol and hydrogen sulfide as follows:



Besides the main reaction, some side reactions may take place as follows [5, 11, 24]:



There is another side reaction, which may sometimes occur in methanol thiolation as follows [10]:



Dimethyl disulfide, (CH<sub>3</sub>)<sub>2</sub>S<sub>2</sub>, is produced in small amounts [26] and can be neglected. DMS, (CH<sub>3</sub>)<sub>2</sub>S, is the main side product produced in three different reactions. The desired product's selectivity is strongly dependent on the catalyst's acid-base properties [15, 19].

The conversion of hydrogen sulfide together with the selectivity and yield of methanethiol and DMS were determined for three catalysts and summarized in Tables 7 and 8 and Figures 7 and 8. The selectivity is defined as the ratio of the desired product to converted hydrogen sulfide. The yield is defined as the ratio of the desired product to the initial amount of hydrogen sulfide. The following relations define conversion, selectivity, and yield:

$$X_{\text{H}_2\text{S}} = \frac{n_{\text{H}_2\text{S},0} - n_{\text{H}_2\text{S}}}{n_{\text{H}_2\text{S},0}} \quad (10)$$

$$S_i = \frac{n_i}{n_{H_2S,0} - n_{H_2S}} \quad (11)$$

$$Y_i = \frac{n_i}{n_{H_2S,0}} \quad (12)$$

**Table 7.** Activity, selectivity, and yield in the case of pure H<sub>2</sub>S as feed

Catalyst	H <sub>2</sub> S conv. %	Selectivity %		Yield %	
		MM	DMS	MM	DMS
A	97.1	0.08	99.9	0.08	97
B	86.7	0.87	99.13	0.75	85.95
C	87.8	1.3	98.7	1.1	86.7

**Table 8.** Activity, selectivity, and yield in the case of acid gas as feed

Catalyst	H <sub>2</sub> S conv. %	Selectivity %		Yield %	
		MM	DMS	MM	DMS
A	78.6	4.94	95	3.8	74.8
B	73.1	3.3	96.7	2.4	70.7
C	63.9	8.5	91.5	5.4	58.5
( $\gamma$ -Al <sub>2</sub> O <sub>3</sub> )	87.0	0.02	0.98	0.02	86.9

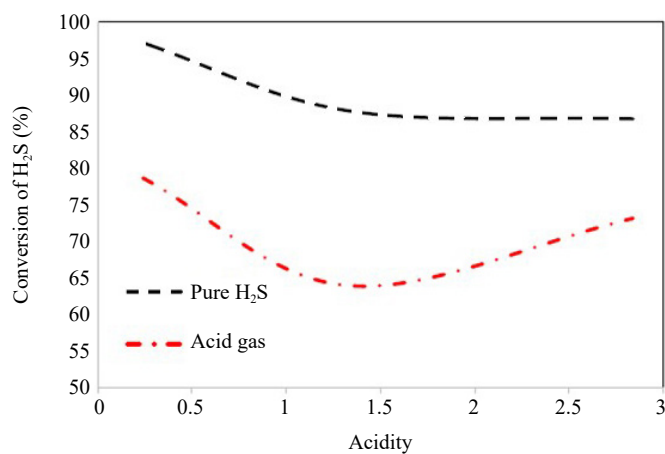


**Figure 7.** Conversion of H<sub>2</sub>S for catalyst's acidity

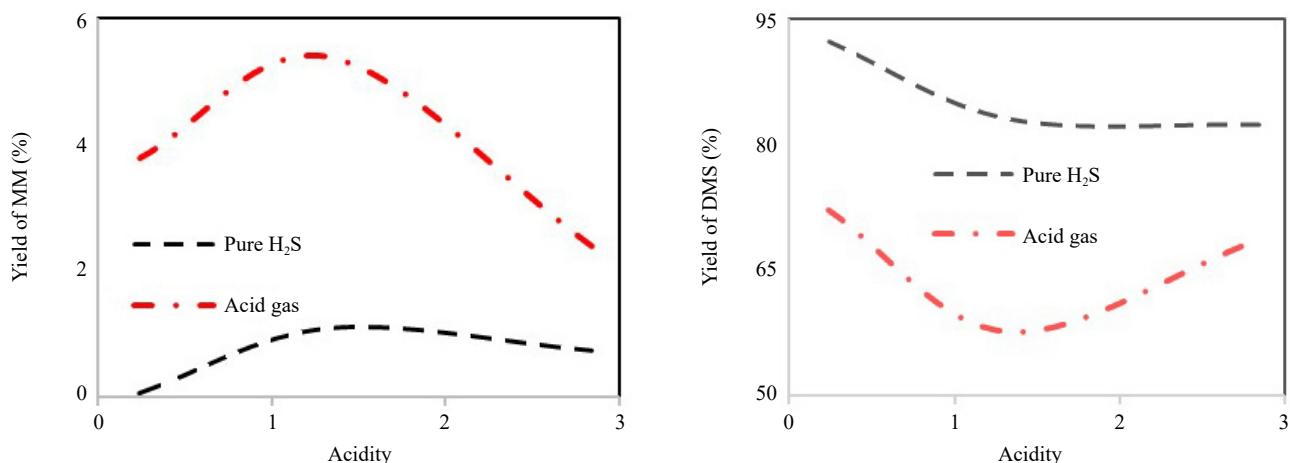


**Figure 8.** The yield of methanethiol (left) and DMS (right) for the catalyst's acidity

Where:  $X_{H_2S}$  is the conversion of  $H_2S$ ,  $n_{H_2S}$  is the mole number of remaining  $H_2S$ ,  $n_{H_2S,0}$  is the initial mole number of  $H_2S$ .  $S_i$  is the selectivity of component  $i$ ,  $n_i$  is the mole number of component  $i$ , and  $Y_i$  is the yield of component  $i$ .  $H_2S$  converts more than 86% in pure  $H_2S$  feed, and catalyst A, with 97.1% conversion shows the best results. The conversion for acid gas feed is in the range of 63.9% to 78.6%. The results also show that all catalysts in both feeds are selective for DMS. The selectivity for DMS is more than 98.7% and 91.5% for pure  $H_2S$  and acid gas feed, respectively.

### 6.3 Products distribution relation with catalyst acidity

The acid-base properties of catalysts play an important role in product distribution in methanol thiolation reactions [16]. Comparing the conversion and yield of products with the catalyst's acidity shows that for both feeds, the conversion of  $H_2S$  has a decreasing trend as the acidity of catalysts increases (Figure 7). The results show that the conversion of  $H_2S$  in pure feed is higher at about 18 units on average than for acid gas feed.

The yield of methanethiol has a maximum at middle acidity. The yield of DMS has a maximum yield at low acidity but a minimum at middle acidity (Figure 8).

### 6.4 Hydrogen production

Exited gas stream from the caustic wash column was sent to GC. Hydrogen and hydrocarbon components showed some peaks on the GC spectrum. The volume percent of hydrogen and hydrocarbons is shown in Tables 9 and 10 for pure  $H_2S$  and acid gas feeds, respectively.

**Table 9.** The volume percent of hydrogen and methane in the reactor outlet with pure  $H_2S$  feed

Catalyst	$H_2$	Methane	Total hydrocarbons
		vol. (%)	
A	8e-3	0.0	0.0
B	1.86	0.3	0.6
C	1.87	0.36	0.77

**Table 10.** The volume percent of hydrogen and hydrocarbons in the reactor outlet with the acid gas feed

Catalyst	H <sub>2</sub>	Methane	Ethane	Propane	i-Butane	n-Butane	Total hydrocarbons
	vol. (%)						
A	62.2	5	5.4	4.4	0.9	2.8	18.6
B	64.1	4.7	5.4	4.5	0.9	1.8	17.5
C	63.2	6	6.4	5.1	1.0	1.8	20.5

A comparison of the mass flow rates of hydrogen and hydrocarbons at the inlet and outlet of the reactor shows an increase for hydrogen of more than 200% and a decrease for hydrocarbons of about 20% (Table 11).

**Table 11.** The mass flow rate of hydrogen and hydrocarbons in the reactor with the acid gas feed

Catalyst	H <sub>2, in</sub>	HC <sub>2, out</sub>	HC <sub>3, in</sub>	HC <sub>4, out</sub>	H <sub>2</sub> increasing (%)	HC decreasing (%)
	(g/min)*10 <sup>3</sup>					
A	3.2	9.8	63.4	51.3	209	19.2
B	3.0	10.1	59.3	46.7	241	21.2
C	2.7	8.1	53.5	43.4	204	18.8

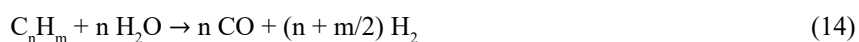
Since the production of hydrogen with a pure H<sub>2</sub>S feed is negligible (Table 9), significant production of hydrogen with an acid gas feed does not relate to reactions 7 and 8.

On the other hand, since hydrocarbons don't play any role in methanol thiolation reactions [9], the reduction of hydrocarbons in the reactor output can be due to the absorption of part of it in caustic solution and the participation of another part in other possible reactions.

It seems other reactions may play a role in the production of hydrogen. The most likely reaction is the pre-reforming of hydrocarbons to produce hydrogen. Steam (H<sub>2</sub>O) is produced during the methanol thiolation reactions series (reactions 1, 2, 3, 5, and 6).

A pre-reformer is usually positioned upstream of the main steam reformer and uses a catalyst with a high nickel content to reform methane and heavier hydrocarbons.

Three reactions occur in the pre-reformer, including steam reforming, water gas shift, and methanation reactions, as follows:



Liquefied petroleum gas is usually referred to as pre-reformer feed. Pre-reforming of propane was studied over an industrial nickel-chromium catalyst under pressures of 1 and 5 atm in the temperature range of 220-380 °C [27]. Hydrogen production via n-butane steam reforming was investigated on Ni/δ-Al<sub>2</sub>O<sub>3</sub> and Pt-Ni/δ-Al<sub>2</sub>O<sub>3</sub> catalysts at temperatures between 305 and 405 K and atmospheric pressure [28].

Therefore, although nickel and platinum catalysts based on alumina are well-known reforming catalysts, the results of this paper show that potassium and tungsten catalysts based on gamma alumina are also able to produce hydrogen during the hydrocarbon reforming process.

## 7. Economic evaluation

To show the economic attractiveness of the proposed process, a conventional sulfur recovery unit (SRU) on an industrial scale was studied for comparison. Conventional SRU consists of Amine and Claus units with elemental sulfur as the final product. The New configuration consists of a methanol thiolation unit and separation units (distillation). Catalyst A was selected due to its highest H<sub>2</sub>S conversion. The unreacted H<sub>2</sub>S is separated in an Amine unit and returned to the feed. Methanethiol, DMS, and light hydrocarbons are the products in the new configuration (Figure 9).

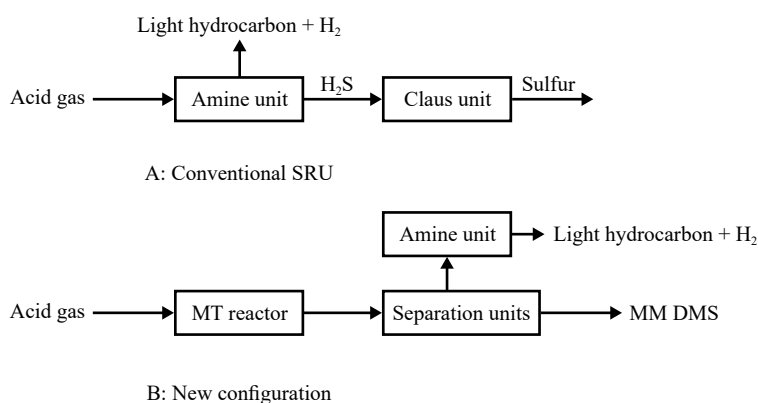


**Figure 9.** Configuration of conventional SRU (A) and proposed process (B). MT: Methanol thiolation, MM: Methanethiol, DMS: Dimethyl sulfide

To calculate the financial parameters, the following assumptions were made: two years for the construction period, 20 years for the production period, a tax rate of 25% of sales with five years of holiday, financing was scheduled 100% by equity, 330 days/year was considered, the discounting rate was 10%, and the capacity of acid gas was 100 ton/day.

Capital costs were estimated from the archives of industrial projects for Amine and Claus units in Research Institute of Petroleum Industry (RIPI). The equipment factored estimation method [29-31] was used for capital cost estimation of the methanol thiolation unit. The capital cost is estimated at 15.7 MMUS\$ for the methanol thiolation unit and 66.6 MMUS\$ for Amine and Claus units.

Operating costs include the cost of raw materials, catalysts, utilities, spare parts, maintenance, labor, labor overhead, insurance, and marketing. It is calculated at 10.5 MMUS\$ and 16 MMUS\$ annually for conventional SRU and the new configuration, respectively.

Sales revenue for conventional SRU has been calculated at 4 MMUS\$ annually. The product is elemental sulfur in an amount of 3.8 tph at a unit cost of 130 \$/ton. Sales for new configurations are calculated at 60.8 MMUS\$ annually. The products are methanethiol and DMS. Methanethiol produces an amount of 0.22 tph at a unit cost of 1000 \$/ton. DMS produces an amount of 5.7 tph at a unit cost of 1000 \$/ton. Since the produced hydrogen needs more purification, hydrogen and hydrocarbons cannot be considered saleable products in the economic evaluation of this study.

Financial parameters were derived, and the results show that an infeasible process can be replaced with another economically feasible one (Table 12).

**Table 12.** Financial parameters of two scenarios

Parameter	Conventional SRU	New configuration
Capital cost (MMUS\$)	66.6	15.7
Operating cost (MMUS\$/yr)	10.4	15.9
Sales revenue (MMUS\$/yr)	4.0	60.8
IRR%	-	156
Dynamic payback period (year)	-	0.4

## 8. Discussion

The presence of hydrogen and hydrocarbons in the acid gas feed causes a reduction in the conversion rate of the hydrogen sulfide. Hydrocarbons can participate in the reforming reactions and produce hydrogen, so some of the active sites of the catalyst may be involved in the reforming reactions and, of course, cannot be available for dissociative adsorption of hydrogen sulfide. Therefore, part of the hydrogen sulfide remains unreacted in the environment.

The presence of hydrogen and CO in the reaction medium provides syngas, which, along with unreacted hydrogen sulfide, can be considered raw materials for the production of methanethiol by utilizing its catalyst and process conditions in future works.

## 9. Conclusion

An acid gas stream containing H<sub>2</sub>S (12.2 mol%, hydrogen, and light hydrocarbons (C<sub>1</sub>-C<sub>4</sub>)) is taken as a source of H<sub>2</sub>S in the methanol thiolation process. Three catalysts of K<sub>2</sub>O/WO<sub>3</sub>/Al<sub>2</sub>O<sub>3</sub> with different loadings of K and W were prepared and tested in a fixed-bed reactor. The best results were related to the catalyst with the lowest acidity (catalyst A). This catalyst gave a maximum conversion of hydrogen sulfide of about 78.6%, which led to the synthesis of methanethiol and DMS. Hydrocarbons participated in the reforming reaction, which led to the production of hydrogen. The reforming reaction took place with the catalyst and under the conditions of the methanol thiolation reaction. The water required for the reforming reaction is supplied by the methanol thiolation reaction. It concluded that the acid gas feed converted to methanethiol, DMS, and hydrogen in reaction with methanol at 360 °C, atmospheric pressure, and the presence of a catalyst. It shows that even without considering hydrogen as a saleable product, the methanol thiolation process with acid gas feedstock can be an economically viable alternative to the conventional sulfur recovery (Claus) process. The unreacted hydrogen sulfide can be recycled to the reactor feed after separation in an amine unit or process with produced syngas to synthesize methanethiol in another reactor with its catalyst and process conditions that can be studied in future works. In addition, replacing K with Rb or Cs and increasing the pressure of the methanol thiolation reaction with acid gas feed can be options for the next work.

Generalizing the results of the effect of acidity from only three catalysts cannot seem reasonable, so to get better results, synthesizing more catalysts with equal acidity or involving the textural properties of the catalysts in future works is recommended.

As the results show, (CH<sub>3</sub>)<sub>2</sub>S is obtained as the main product, but using core-shell catalysts can increase the selectivity of CH<sub>3</sub>SH. A molecular sieve (ZSM-5) in the core and a metal oxide in the shell helps to increase the yield of methanethiol [32, 33].

## Acknowledgment

The authors would like to thank the people in RIPI's refining laboratory for their support, without whose help this work would never have been possible.

## Conflict of interest

The authors would like to thank the people in RIPI's refining laboratory for their support, without whose help this work would never have been possible.

## References

- [1] Song C. An overview of new approaches to deep desulfurization for ultra-clean gasoline, diesel fuel and jet fuel. *Catalysis Today*. 2003; 86(1-4): 211-263. Available from: [https://doi.org/10.1016/S0920-5861\(03\)00412-7](https://doi.org/10.1016/S0920-5861(03)00412-7).

- [2] Srivastava VC. An evaluation of desulfurization technologies for sulfur removal from liquid fuels. *RSC Advances*. 2012; 2(3): 759-783. Available from: <https://doi.org/10.1039/C1RA00309G>.
- [3] Eow JS. Recovery of sulfur from sour acid gas: A review of the technology. *Environmental Progress*. 2002; 21(3): 143-162. Available from: <https://doi.org/10.1002/ep.670210312>.
- [4] Gupta AK, Ibrahim S, Al Shoaibi A. Advances in sulfur chemistry for treatment of acid gases. *Progress in Energy and Combustion Science*. 2016; 54: 65-92. Available from: <https://doi.org/10.1016/j.pecs.2015.11.00>
- [5] Folkins HO, Miller EL. Synthesis of mercaptans. *Industrial & Engineering Chemistry Process Design and Development*. 1962; 1(4): 271-276. Available from: <https://doi.org/10.1021/i260004a007>.
- [6] Ponceblanc H, Tamburro F. *Process for the preparation of methyl mercaptan*. 5847223 (Google Patent) 1998.
- [7] Cook CM, Albright DE, Savidakis MC. *Synthesis of mercaptans from alcohols*. 5874630 (Google Patent) 1999.
- [8] Möller A, Böck W, Rautenberg S, Hasselbach HJ, Taugner W, Heinzl H, et al. *Method for the separation of methyl mercaptan from reaction gas mixtures*. US7199270B2 (Google Patent) 2007.
- [9] Brand A, Quaschnig V. *Catalyst for the production of methyl mercaptan from methanol and hydrogen sulfide*. US7687667B2 (Google Patent) 2010.
- [10] Fonfe B, Fuß S, Wilz F, Jakob H, Weckbecker C. *Catalyst for the synthesis of alkyl mercaptans and process for producing it*. US9764309B2 (Google Patent) 2017.
- [11] Pashigreva AV, Kondratieva E, Bermejo-Deval R, Gutiérrez OY, Lercher JA. Methanol thiolation over  $\text{Al}_2\text{O}_3$  and  $\text{WS}_2$  catalysts modified with cesium. *Journal of Catalysis*. 2017; 345: 308-318. Available from: <https://doi.org/10.1016/j.jcat.2016.11.036>.
- [12] Bermejo-Deval R, Walter RM, Gutiérrez OY, Lercher JA. On the role of the alkali cations on methanol thiolation. *Catalysis Science & Technology*. 2017; 7(19): 4437-4443. Available from: <https://doi.org/10.1039/C7CY01255A>.
- [13] Chen S, Zhang Y, Lin L, Jing X, Yang Y.  $\text{K}_2\text{WO}_4/\text{Al}_2\text{O}_3$  catalysts for methanethiol synthesis from methanol and  $\text{H}_2\text{S}$ : Effect of catalyst preparation procedure. *Reaction Kinetics, Mechanisms and Catalysis*. 2019; 127(2): 917-930. Available from: <https://doi.org/10.1007/s11144-019-01614-9>.
- [14] Weber-Stockbauer M, Gutiérrez OY, Bermejo-Deval R, Lercher JA. The role of weak Lewis acid sites for methanol thiolation. *Catalysis Science & Technology*. 2019; 9(2): 509-516. Available from: <https://doi.org/10.1039/C8CY02250J>.
- [15] Weber-Stockbauer M, Gutiérrez OY, Bermejo-Deval R, Lercher JA. Cesium induced changes in the acid-base properties of metal oxides and the consequences for methanol thiolation. *ACS Catalysis*. 2019; 9(10): 9245-9252. Available from: <https://doi.org/10.1021/acscatal.9b02537>.
- [16] Shabani MR, Moosavian MA, Zamani Y, Royaei SJ. Effect of acid-base properties on design of catalyst for methanol thiolation: A review. *Comptes Rendus. Chimie*. 2020; 23(6-7): 433-444. Available from: <https://doi.org/10.5802/crchim.45>.
- [17] Mul G, Wachs IE, Hirschon AS. Catalytic synthesis of methanethiol from hydrogen sulfide and carbon monoxide over vanadium-based catalysts. *Catalysis Today*. 2003; 78(1-4): 327-337. Available from: [https://doi.org/10.1016/S0920-5861\(02\)00309-7](https://doi.org/10.1016/S0920-5861(02)00309-7).
- [18] Chen A, Wang Q, Li Q, Hao Y, Fang W, Yang Y. Direct synthesis of methanethiol from  $\text{H}_2\text{S}$ -rich syngas over sulfided Mo-based catalysts. *Journal of Molecular Catalysis A: Chemical*. 2008; 283(1-2): 69-76. Available from: <https://doi.org/10.1016/j.molcata.2007.12.014>.
- [19] Huang S, He S, Deng L, Wang J, He D, Lu J, Luo Y. One-step Synthesis of methanethiol with mixture gases ( $\text{CO}/\text{H}_2\text{S}/\text{H}_2$ ) over SBA-15 supported Mo-based catalysts. *Procedia Engineering*. 2015; 102: 684-691. Available from: <https://doi.org/10.1016/j.proeng.2015.01.166>.
- [20] Cordova A, Blanchard P, Lancelot C, Frémy G, Lamonier C. Probing the nature of the active phase of molybdenum-supported catalysts for the direct synthesis of methylmercaptan from syngas and  $\text{H}_2\text{S}$ . *ACS Catalysis*. 2015; 5(5): 2966-2981. Available from: <https://doi.org/10.1021/cs502031f>.
- [21] Cordova A, Blanchard P, Salembier H, Lancelot C, Frémy G, Lamonier C. Direct synthesis of methyl mercaptan from  $\text{H}_2/\text{CO}/\text{H}_2\text{S}$  using tungsten based supported catalysts: Investigation of the active phase. *Catalysis Today*. 2017; 292: 143-153. Available from: <https://doi.org/10.1016/j.cattod.2016.10.032>.
- [22] Lu J, Luo Y, He D, Xu Z, He S, Xie D, et al. An exploration into potassium (K) containing  $\text{MoS}_2$  active phases and its transformation process over  $\text{MoS}_2$  based materials for producing methanethiol. *Catalysis Today*. 2020; 339: 93-104. Available from: <https://doi.org/10.1016/j.cattod.2019.01.012>.
- [23] Yu M, Kosinov N, Van Haandel L, Kooyman PJ, Hensen EJ. Investigation of the active phase in K-promoted  $\text{MoS}_2$  catalysts for methanethiol synthesis. *ACS Catalysis*. 2020; 10(3): 1838-1846. Available from: <https://doi.org/10.1021/acscatal.9b03178>.
- [24] Yermakova A, Mashkina A. Kinetic model of the reaction of methanol with hydrogen sulfide. *Kinetics and Catalysis*.

2004; 45(4): 522-529. Available from: <https://doi.org/10.1023/B:KICA.0000038080.28824.f8>.

- [25] Paglia G. *Determination of the structure of  $\gamma$ -alumina using empirical and first principle calculations combined with supporting experiments*. PhD thesis. Curtin University; 2004.
- [26] Calvino-Casilda V, Martin-Aranda R, Sobczak I, Ziolek M. Modification of acid-base properties of alkali metals containing catalysts by the application of various supports. *Applied Catalysis A: General*. 2006; 303(1): 121-130. Available from: <https://doi.org/10.1016/j.apcata.2006.02.013>.
- [27] Uskov SI, Potemkin DI, Enikeeva LV, Snytnikov PV, Gubaydullin IM, Sobyanin VA. Propane pre-reforming into methane-rich gas over Ni catalyst: Experiment and kinetics elucidation via genetic algorithm. *Energies*. 2020; 13(13): 3393. Available from: <https://doi.org/10.3390/en13133393>.
- [28] Avcı AK, Trimm DL, Aksoylu AE, Önsan ZI. Hydrogen production by steam reforming of n-butane over supported Ni and Pt-Ni catalysts. *Applied Catalysis A: General*. 2004; 258(2): 235-240. Available from: <https://doi.org/10.1016/j.apcata.2003.09.016>.
- [29] Peters MS, Timmerhaus KD, West RE. *Plant design and economics for chemical engineers*. 5th ed. New York, United States: McGraw Hill; 2003.
- [30] Shabani MR, Yekta RB. Suitable method for capital cost estimation in chemical processes industries. *Cost Engineering*. 2006; 48(5): 22-25. Available from: <https://doi.org/10.13140/RG.2.1.1545.7762>.
- [31] Shabani MR, Moosavian MA, Royaei SJ, Zamani Y. Methanol thiolation: A feasible process solution for H<sub>2</sub>S recovery in refineries. *International Journal of Oil, Gas and Coal Technology*. 2021; 28(4): 486-505. Available from: <https://doi.org/10.1504/IJOGCT.2021.118809>.
- [32] Liu P, Cao J, Xu Z, Yang C, Wang X, Liu F. Thiolation of methanol with H<sub>2</sub>S using core-shell structured ZSM-5@t-ZrO<sub>2</sub> catalyst. *Chemical Engineering Science*. 2020; 211: 115273. Available from: <https://doi.org/10.1016/j.ces.2019.115273>.
- [33] Wang Y, Yang T, Liu F, Zhao T, Wang X, Cao J. High selectivity in methanethiol synthesis over a coated composite comprising ZSM-5 with t-ZrO<sub>2</sub>. *Microporous and Mesoporous Materials*. 2020; 305: 110358. Available from: <https://doi.org/10.1016/j.micromeso.2020.110358>.